

# A 2 GHz Surface Transverse Wave Oscillator with Low Phase Noise

LUDWIG EICHINGER, STUDENT MEMBER, IEEE, BERND FLEISCHMANN,  
 PETER RUSSER, SENIOR MEMBER, IEEE, AND  
 ROBERT WEIGEL, STUDENT MEMBER, IEEE

**Abstract**—A hybrid oscillator at 1.9805 GHz has been developed using acoustic surface transverse wave (STW) delay lines operating at the third harmonic as the frequency controlling element. The STW delay lines were fabricated on 37.5° rotated Y-cut quartz substrates with a photolithographic technique. A very thin metallization (25 nm) was used to obtain low insertion loss. A split isolated electrode design was used for the transducers. The  $Q$  value and the untuned insertion loss of the STW filter were 3400 and 21 dB, respectively. The phase noise and temperature stability of the oscillator were characterized. At a power output of 6.5 dBm a single-sideband phase noise to carrier ratio of  $-100$  dBc/Hz at 1 kHz was attained.

## I. INTRODUCTION

**I**N THE GIGAHERTZ range surface acoustic wave (SAW) delay line oscillators are being developed for a wide variety of commercial and military applications, including radar, satellite communications, telemetry, gigabit logic using GaAs and Josephson junctions, and navigation. Phase noise specifications have been pushed to extremely low noise levels. Direct generation of frequencies minimizes multiplication and avoids phase noise increase due to the multiplication process. A significant advantage of SAW controlled frequency sources over other oscillators is the very low FM noise level which can be achieved [1]. By using piezoelectric Rayleigh waves, the upper frequency limit is approximately 1.2 GHz due to the limitations of the fabrication process if standard optical lithography production methods are employed. By operating at a higher harmonic, the frequency range can be extended up to 2 GHz, but conversion of the Rayleigh waves to acoustic bulk waves increases the insertion loss and reduces the maximally achievable  $Q$  value [2]. The use of surface transverse waves (STW's) on AT-cut quartz substrates hav-

ing a 60 percent higher propagation velocity and smaller mode conversion losses than the common Rayleigh waves shifts the frequency limit to above 3 GHz when operating at a higher harmonic [3].

In this work, a high-performance 1.9805 GHz STW delay line oscillator is described, and its performance analyzed. The key element of the device is the STW delay line, controlling the frequency of oscillation, the tuning bandwidth, and the stability of the oscillator. Thin-film technology offers flexibility of design for optimizing the STW filter in each oscillator application. The filter characteristics are mainly determined by transducer length and electrode spacing, while the delay is given by the separation of the two transducers. The characteristics of the STW delay line are determined by the architecture of the transducer structures. Using computer-aided design methods, described in Section III, the frequency response of the filter is predictable, thus permitting its optimization. To complete the oscillator, the STW filter is then integrated into a hybrid circuit, presented in Section II. The oscillator performance is given in Section IV. Phase noise is the predominant factor of short-term stability. It is due to random phase modulation of the carrier frequency produced by white noise and  $1/f$  noise sources in the oscillator loop. A low level of close to carrier phase noise is desirable for applications in wide-dynamic-range communication systems. It is also of interest in radar systems where information contained in a Doppler shift can be obscured and in digital communication systems where accurate timing is essential. Commonly, the phase noise of SAW oscillators, which has been examined by a number of authors [4]–[7], is viewed in the frequency domain. Here, for convenience, Parker's theory [5] will be used. The temperature stability of the frequency of the STW oscillator is largely controlled by the temperature behavior of the filters' substrate material. Experimental frequency versus temperature curves of three different cuts of quartz substrates are given. The oscillator described here was designed for a turnover temperature of approximately 80°C. The electronic components of an oscillator tend to shift the turnover point to lower temperatures. Thus, a 37.5° rotated Y-cut quartz substrate, which has a turnover tem-

Manuscript received April 11, 1988; revised August 29, 1988.

L. Eichinger was with the Lehrstuhl für Hochfrequenztechnik, Technische Universität München, München 2, West Germany. He is now with Work Microwave GmbH, D-8150 Holzkirchen, West Germany.

B. Fleischmann is with the Siemens Research Laboratories München, D-8000 München 83, West Germany.

P. Russer and R. Weigel are with the Lehrstuhl für Hochfrequenztechnik, Technische Universität München, D-8000 München 2, West Germany.

IEEE Log Number 8824339.

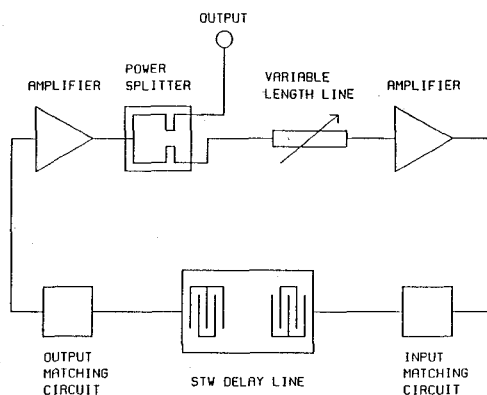


Fig. 1. STW oscillator block diagram schematic.

perature of about  $83^{\circ}\text{C}$ , was employed. The temperature behavior of the uncompensated oscillator is discussed.

## II. OSCILLATOR CIRCUIT

The construction of the STW oscillator is very similar to the SAW delay line oscillator. The block diagram is shown schematically in Fig. 1. The components include the STW delay line, amplifiers, phase shifter, matching networks, and output coupler. The frequency of oscillation is determined by the frequency of the STW device in the feedback loop, which in our case is 1.9805 GHz. The small-signal gain of the amplifiers at the frequency of oscillation must be greater than the loss associated with the delay line and any other loop components. In our hybrid design we use two identical silicon bipolar low-noise MMIC amplifiers with a gain of 17.7 dB at 2 GHz. In order to achieve a low phase noise the STW delay line must have low insertion loss and high  $Q$  [8]. The design of the delay lines is described in more detail in Section III. The phase around the loop has to be an integral number of  $2\pi$  radians. As a phase shifter a variable length line is used which, like the remaining components, has been fabricated in softboard microstrip technology ( $\epsilon = 10.5$ ). The dimensions of the substrate are 1 in  $\times$  2 in. The output coupler is a 3 dB Wilkinson power divider [9]. No output buffer amplifier was used.

The computer-aided design and optimization of the complete circuit, including microstrip Wilkinson power splitter, matching networks, and variable length line, were done by using a standard microwave simulation and optimization program [10]. The design has the advantage that the output impedance of the amplifiers lies close to  $50 \Omega$ . Both the input impedance and the output impedance of the delay line have a real value of approximately  $20 \Omega$ . For purposes of simulation and measurement, the oscillator loop has been opened between the variable length line and the following amplifier. By terminating the two open ports with their correct impedances required for closed-loop operation, in order to satisfy the oscillation condition, an open-loop design was performed. Fig. 2 shows the measured open-loop gain (upper trace) and phase shift (lower trace). The gain of the amplifiers is large enough to provide a positive loop gain of 4 dB and is flat over the

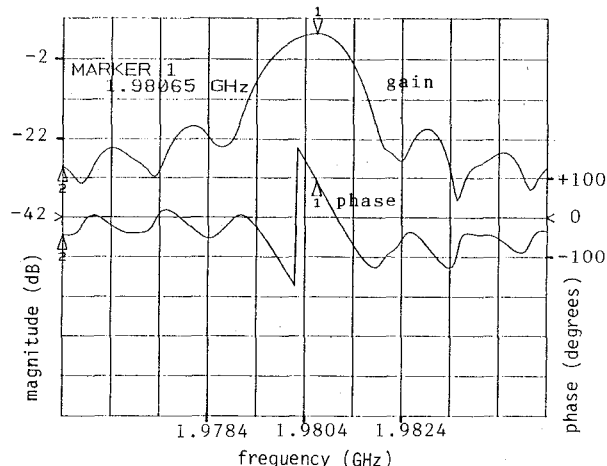


Fig. 2. Open-loop gain and phase of the 1.9805 GHz STW delay line oscillator.

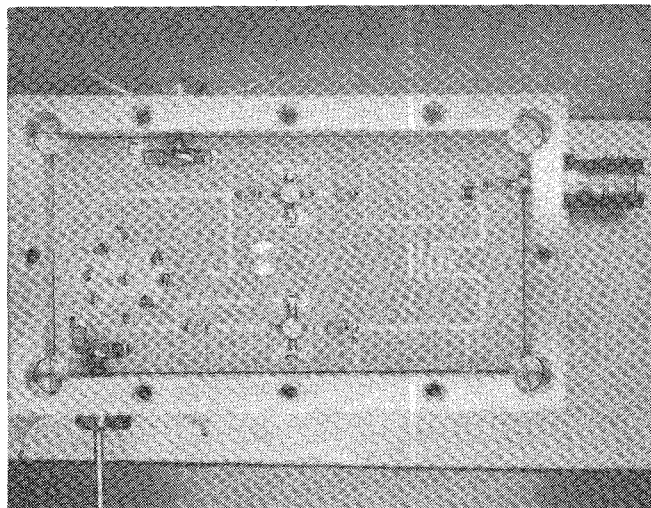


Fig. 3. 1.9805 GHz STW delay line oscillator.

frequency range of interest. If the loop is closed, oscillation starts, and the signal amplitude increases until one of the amplifiers saturates and the loop gain is reduced to 0 dB. The equilibrium power level of the oscillator is then the 4 dB compression point of the amplifier chain. By changing the total phase shift through the circuit with a short microstrip transmission line, the oscillator can be made to operate over nearly the entire frequency range of positive open-loop gain. By properly adjusting the length of the phase-shifting microstrip line, we obtained an oscillation frequency of 1.9805 GHz. The oscillator has a power output of 6.5 dBm, and the load pulling (frequency stability) has been measured to be 41 kHz at 12 dB return loss. A photograph of the oscillator is included as Fig. 3.

## III. STW DELAY LINE DESIGN AND FABRICATION

The main advantages of using STW on quartz substrates instead of piezoelectric Rayleigh waves are the high propagation velocity on AT-cut quartz and the zero coupling of other modes [11], [12]. For low-noise single-mode oscillator

applications the design parameters of the STW delay lines are mainly insertion loss and  $Q$  value [13].

#### A. Analysis Method and STW Delay Line Design

The STW delay lines were designed with highly advanced analysis methods. A model has been used which considers the effect of the electrostatic charge distribution on the finger electrodes of the interdigital electroacoustic transducers. For the analysis of harmonic responses the transducer is split up into a series of basic elements. These elements are delay lines in order to simulate acoustic surface wave propagation on the free and the metallized substrate, step discontinuities to account for acoustic reflections at the finger edges, and piezoelectric excitation cells.

To calculate the excitation strength of the STW at arbitrary harmonics it is necessary to know the electrostatic charge distribution on the transducer. A Green's function method was applied to calculate the electrostatic charge distribution of an arbitrary transducer structure including floating electrodes [14]. Each electrode is divided into  $n$  substrips of different widths  $l_n$ . The mean charge densities  $\sigma_n$  are calculated for each substrip  $n$  of all the electrodes of the transducer. The amplitude of the excited acoustic surface wave is given by [15]

$$a_n = C \sigma_n l_n \frac{\sin(kl_n/2)}{kl_n/2} \quad (1)$$

where  $C$  is composed of material coefficients and of the acoustic wavenumber  $k$ . A superposition of these partial waves results in the amplitude of the excited wave from the  $m$ th electrode

$$A_m = \sum a_n \exp[j(x_n - x_m)] \quad (2)$$

and the scattering matrix of the excitation cell can now be constructed [16]. The acoustic reflection elements of the model are described in detail elsewhere [17].

By cascading the scattering matrices of all the basic elements the transfer function of the transducer is obtained. It should be noted that this method of analysis was developed for Rayleigh wave delay lines, but it also gives accurate results for STW delay lines if the conversion of STW to bulk shear waves, which occurs at higher harmonics, is considered as propagation loss.

With this analysis method the excitation strength at harmonic frequencies can be calculated very accurately. The relative coupling coefficient  $k_r^2$  is defined by

$$k_r^2 = \frac{G(f_j)}{N_j k_0^2 2\pi f_j C_T} \quad (3)$$

where  $N_j$  is the transducer length in wavelengths at the harmonic frequency  $f_j$ ,  $k_0^2$  the coupling coefficient of the substrate,  $G(f_j)$  the transducer radiation conductance, and  $C_T$  the capacitance. The relative coupling coefficient  $k_r^2$  is a useful measure for the excitation strength at harmonic frequencies [3]. It has been found to be highly insensitive to the metallization ratio. A higher  $k_r^2$  corresponds to a

better coupling of the STW. The piezoelectric coupling of the STW increases with increasing layer thickness, even at frequencies above the stopband frequency of the grating which is formed by the transducer [18]. Conversion to shear horizontal bulk waves at the edges of the electrodes cannot be prevented. So the STW is similar to a leaky surface wave. The similarity of the STW to the bulk shear wave directly above the stopband frequency [19] may be attributed to the peak in the mode conversion ratio at the so-called enter frequency  $f_e$ , which is given by [20]

$$f_e = \frac{v_s v_b}{p(v_s + v_b)} \quad (4)$$

where  $p$  is the grating period,  $v_s$  the velocity of the acoustic surface wave, and  $v_b$  the velocity of the slowest bulk wave which contributes to the surface wave. The enter frequency of the STW, which is slightly slower than the bulk shear wave, is close to the stopband (Bragg) frequency.

In our design we use uniform, i.e., unweighted, transducers with an energy trapping structure [21]. The basic shape of the filter transfer function is therefore a  $[\sin(x)/x]^2$  curve with a nominal sidelobe suppression of 26 dB. By multiple transit signals and propagation loss the sidelobe suppression can be degraded to values near 20 dB, which is still sufficient for oscillator applications. Each delay line consists of two identical split isolated interdigital transducers. In the split isolated transducer type every second electrode is floating, i.e. not connected to the bus bars [22]. Thus, the capacity and the radiation conductance are reduced by half [23]. This allows a reduction of acoustic diffraction effects, which could decrease the maximally achievable  $Q$  value, by doubling the acoustic aperture without significant change of the impedance. Due to the symmetry of the transducer only odd harmonics of the center frequency are excited. Both the fundamental frequency, i.e., one period being one wavelength, and the third harmonic, i.e., one period being three wavelengths, are excited with considerable strength. Higher harmonics are less useful because of weaker coupling and higher sensitivity to line width deviations in the fabrication process. Stray capacitances of the bonding pads and stray magnetic fields of the transducer electrodes and bonding wires may generate high spurious signals and distortions due to electromagnetic feedthrough. But because the phase of the inductive crosstalk depends on the geometry of the structure a destructive interference of both the capacitive and inductive components can be achieved by properly designing the layout of the delay line.

#### B. Fabrication and Delay Line Data

The filters were designed for a third harmonic frequency of 1.98 GHz. Long transducers with a geometric period of 1.926  $\mu\text{m}$  were used to achieve a high  $Q$  value. The delay lines were fabricated on 37.5° rotated Y-cut quartz substrates to achieve a turnover temperature of 83°C. A very thin metallization of 25 nm pure aluminum was applied.

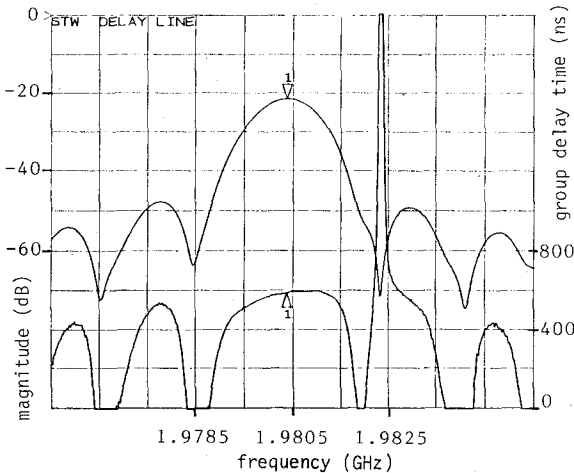


Fig. 4. Frequency response and group delay time of STW delay line.

For high- $Q$  delay lines a thin metallization thickness is indispensable to avoid excessive acoustic mode conversion losses. For example, with an aluminum thickness of 40 nm instead of 25 nm, a 10 dB higher insertion loss has been measured. A standard photolithographic process with 10:1 projection printing and lift-off technique was used. The line width resolution is about 0.8  $\mu$ m. Operation at a higher harmonic provides general benefits on the reproducibility. Frequency deviations will be the same if the relative line width deviations are the same. Thus, using a fundamental frequency design, which has smaller line widths, requires a higher production accuracy to achieve the same scatter of the electrical parameters. To maintain the metallization thickness within only a few hundred picometers over the whole area of the wafer is of great importance for the reproducibility of the frequency. We measured a dependency of the acoustic wave velocity on the thickness of the aluminum layer of approximately 100 ppm/nm. The delay lines are fabricated with high precision and high reproducibility. For measurements which were made with an HP8510B network analyzer, the filters were mounted into standard TO-8 packages with an organic adhesive and bonded with gold wires. We obtain standard deviations for the center frequency of typically 40 ppm and for an insertion loss of 0.4 dB. These data may be improved if the inductance of the bonding wires is controlled more accurately. The delay lines were characterized by a center frequency of 1.9805 GHz, an untuned insertion loss of approximately 21 dB, a 3 dB bandwidth as small as 1.2 MHz to ensure single-mode operation of the oscillator, and a group delay time of 550 ns. The  $Q$  value is measured at approximately 3400, which is very high with respect to a frequency of almost 2 GHz. Both the input impedance and the output impedance have nearly real values of 20  $\Omega$ . Fig. 4 is a plot of the measured frequency response (upper trace) and the group delay time (lower trace) around the third harmonic. As can be seen, the filters' passbands are shaped like  $[\sin(x)/x]^2$ . A broad-band measurement is shown in Fig. 5. The fundamental frequency is at 660

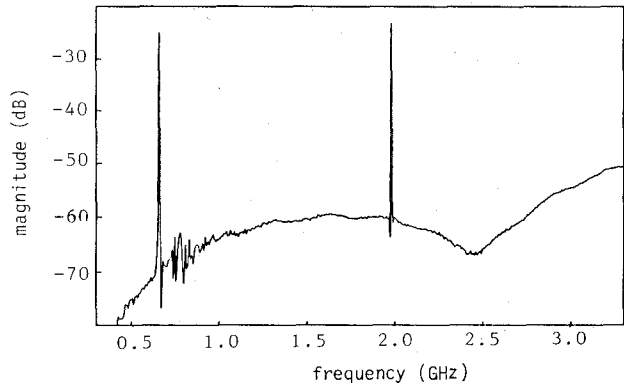


Fig. 5. Broad-band frequency response of STW delay line.

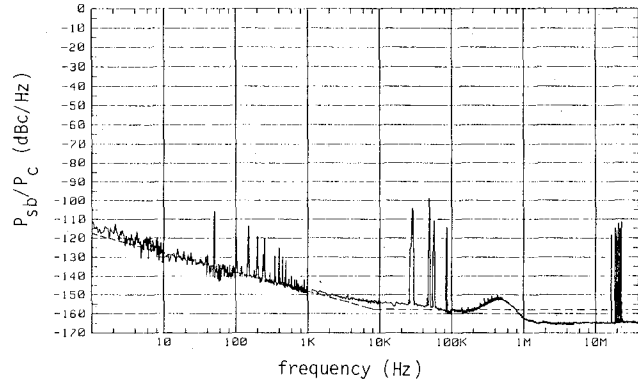


Fig. 6. Phase noise characteristics of STW delay line.

MHz. Only weak spurious responses due to acoustic bulk waves in the 75 MHz region are observed.

#### IV. OSCILLATOR STABILITY

The stability of the oscillator has been investigated in regard to its phase noise (short-term stability) and temperature behavior (medium-term stability). Long-term aging characteristics can be improved, as with SAW oscillators, by removing the dominant aging mechanisms [24].

##### A. Phase Noise

The amplifiers used in the oscillator circuit were commercial silicon bipolar devices which have a very low  $1/f$  noise level. Thus, the STW delay line has been identified as the dominant source of flicker noise. Flicker noise is known to exist in quartz delay lines over the offset frequency range of 10 mHz to 100 kHz [25]. The causes of  $1/f$  noise in delay lines are not well understood. However, it has been proved that the fluctuations of certain transducer parameters can be directly translated to the carrier frequency [26], [27]. No surface treatment with silicone material [5] has been applied to our STW delay lines. Fig. 6 shows the measured (full line) and the calculated (broken line) single-sideband spectral density,  $S_\phi(f_m)/2$ , of the STW delay line. Here  $f_m$  is the frequency of the phase fluctuations,  $\Delta\phi$ . These phase fluctuations appear in the output signal if a noise-free signal is passed through the delay line in series with the amplifiers. The frequency  $f_m$  is

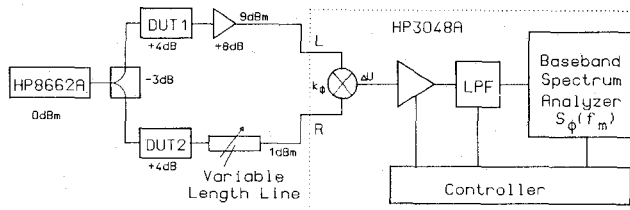


Fig. 7. System for measurement of phase noise of STW delay lines.

referred to as the modulation (Fourier) frequency. The relation

$$(\Delta\phi)^2 = S_\phi(f_m) \quad (5)$$

has been used, where  $(\Delta\phi)^2$  is normalized to a 1 Hz bandwidth. The  $1/f_m$  dependence of the close to carrier noise is clearly seen. The open-loop phase noise,  $L_o(f_m)$ , is described by the expression

$$L_o(f_m) = \frac{\alpha}{2\pi f_m} + \frac{GFkT}{P_c} \quad (6)$$

where  $\alpha$  is a flicker noise parameter determined by the delay line which must be measured experimentally,  $P_c$  the carrier power level,  $G$  the amplifier gain,  $F$  the amplifier noise figure,  $k$  Boltzmann's constant, and  $T$  the temperature. The value of  $f_m$  when  $\alpha/(2\pi f_m) = GFkT/P_c$  is called the flicker frequency,

$$f_\alpha = \frac{\alpha P_c}{2\pi GFkT}. \quad (7)$$

The flicker noise parameter  $\alpha$  and the flicker frequency  $f_\alpha$  are determined experimentally to be  $4.3 \times 10^{-11} \text{ s}^{-1}$  and 8 kHz, respectively.

Measurements were made with an HP3048A noise analyzer using the two STW device phase detector method described in detail elsewhere [28]. The setup for the test system is shown in Fig. 7, which also indicates the actual power levels. The measurement is performed by splitting the signal of a stable HP8662A signal generator into two paths. The paths each contain a STW delay line of very similar frequency, insertion loss, and  $Q$  value. A phase-shifting variable length line is inserted in one of the paths, and a low-noise amplifier is added to the other path in order to saturate the low-noise mixer so that AM noise is suppressed. Adjusting the variable length line such that the two signals at the mixer are in quadrature, the mixer output is proportional to the phase difference between the signals of the two paths. By using this measurement technique it is possible to measure the phase perturbations in the delay line directly and without ambiguity. Fig. 8 is a plot of the system noise floor which has been recorded by replacing the STW delay lines with attenuators of similar insertion loss.

The (closed-loop) delay line oscillator transfer function,  $H(f_m)$ , is described by the expression

$$H(f_m) = 1 + (2\pi f_m \tau)^{-2} \quad (8)$$

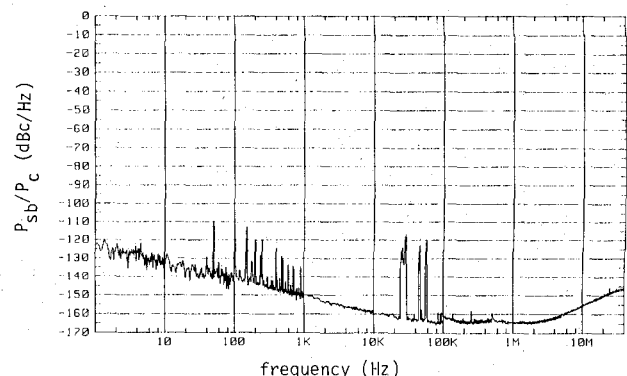


Fig. 8. System noise floor of two STW device phase detector method.

where  $\tau$  is the group delay time of the STW delay line. The relation between  $\tau$  and  $Q$  is given by

$$Q = \pi f \tau. \quad (9)$$

The phase noise of the complete oscillator is obtained by multiplying (6) and (8),

$$L_o(f_m) H(f_m) = \frac{\alpha}{\omega_m^3 \tau^2} + \frac{GFkT}{P_c \omega_m^2 \tau^2} + \frac{\alpha}{\omega_m} + \frac{GFkT}{P_c} \quad (10)$$

where  $\omega_m$  equals  $2\pi f_m$ . The  $1/f_m$  phase noise in the delay line appears as a  $1/f_m^3$  dependence in the phase noise spectral density of the oscillator below the flicker frequency  $f_\alpha$ . Again, a thermal noise floor of  $GFkT/P_c$  for modulation frequencies far away from the carrier is observed. Of the two middle terms of (10) the one that dominates depends on the value of  $f_m$  when  $(\omega_m \tau)^{-2} = 1$ . This frequency is called the oscillator feedback frequency  $f_\tau$  and is equal to

$$f_\tau = \frac{1}{2\pi\tau}. \quad (11)$$

In our case the oscillator feedback frequency  $f_\tau$  equals 280 kHz, hence there is no region of  $1/f_m$  dependence. Thus, it follows from (10) that the phase noise of the STW delay line oscillator,  $S_\phi(f_m)/2$ , which is the ratio of the single-sideband noise power in a 1 Hz bandwidth,  $P_{sb}$ , to the carrier power,  $P_c$ , given in decibels relative to the carrier, can approximately be written as

$$\frac{P_{sb}}{P_c} = 10 \log \left[ \frac{\alpha}{\omega_m^3 \tau^2} + \frac{GFkT}{P_c} \left[ \frac{1}{\omega_m^2 \tau^2} + 1 \right] \right]. \quad (12)$$

Application of this theory to our oscillator yields a theoretical noise floor of  $-158 \text{ dBc/Hz}$ .

Fig. 9 shows the measured single-sideband phase noise spectrum of the (closed-loop) oscillator. Again, measurements were made with an HP3048A noise analyzer, in this case using a frequency discriminator method which does not require an extra reference source [29]. The test system schematic including the power levels is shown in Fig. 10. As a delay line in one of the paths of the measurement setup we use one of our STW delay lines. This delay line will convert the short-term fluctuations of the oscillator

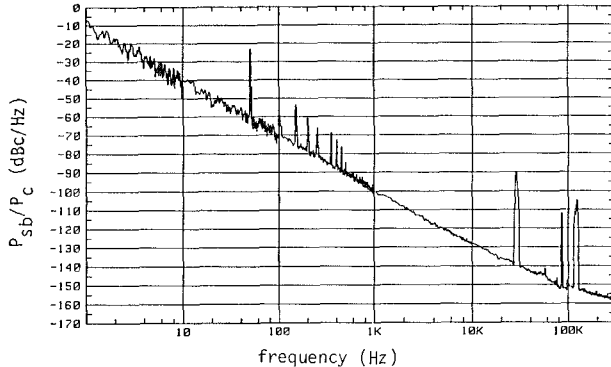


Fig. 9. Single-sideband phase noise of 1.9805 GHz STW delay line oscillator.

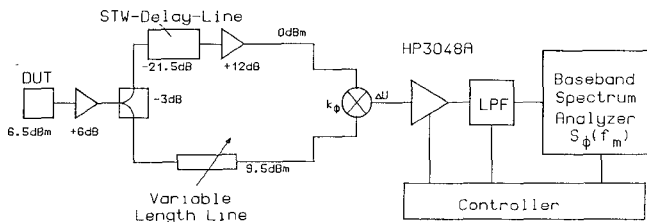


Fig. 10. System for measurement of phase noise of STW delay line oscillators.

into phase fluctuations which are converted, via the low-noise mixer, into voltage fluctuations,  $\Delta U(f_m)$ , that can be measured with a baseband spectrum analyzer. These voltage fluctuations can be expressed in phase noise units using the discriminator constant,  $k_d$ , which is given by the expression

$$k_d = 2\pi\tau k_\phi \frac{\sin(\pi f_m \tau)}{\pi f_m \tau} \quad (13)$$

where  $k_\phi$  is the mixer constant and  $\tau$  the delay time provided by the STW delay line in the upper path of the measurement setup. To avoid having to compensate for the  $\sin(x)/x$  response, measurements are accurate and sensitive only for modulation frequencies  $f_m$  much less than  $1/\tau$ , where the first null of the transfer response occurs. In our case, measurements will become inaccurate for modulation frequencies above 300 kHz.

The phase noise of the STW oscillator is  $-100$  dBc/Hz at 1 kHz and  $-70$  dBc/Hz at 100 Hz.

### B. Temperature Behavior

The overall temperature coefficient of an uncompensated STW delay line oscillator is largely determined by the temperature coefficient of the substrate material which is used for fabrication of the delay lines. Rotated Y-X-cut quartz substrates offer parabolic temperature coefficients of delay with low constants of parabolicity and a wide range of turning point temperatures [30]. This is modified owing to the presence of surface metallization [31], but there is no difficulty in selecting a cut for maximum frequency stability, so that the turning point temperature of the oscillator occurs at the nominal operating tempera-

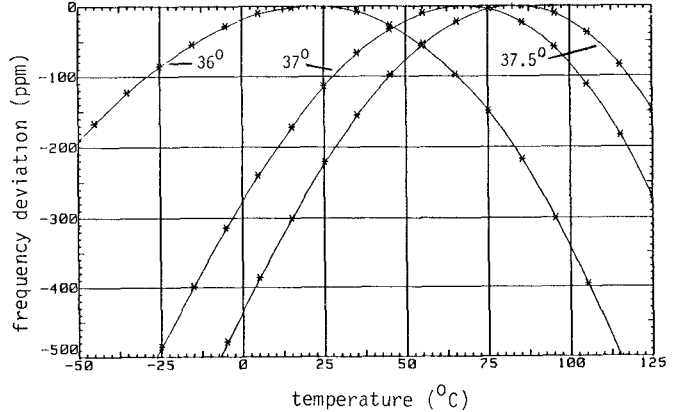


Fig. 11. Frequency versus temperature of STW delay lines.

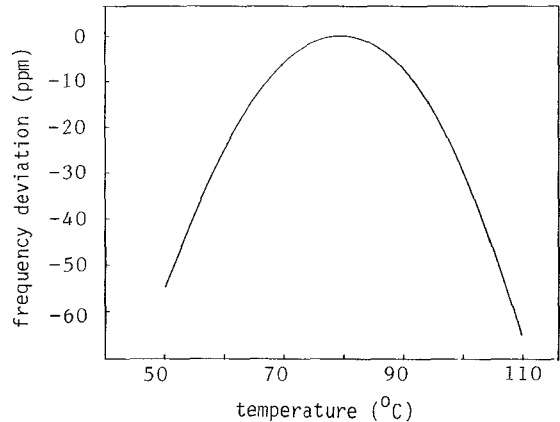


Fig. 12. Frequency versus temperature of 1.9805 GHz STW oscillator.

ture, for maximum frequency stability. Fig. 11 shows the experimental temperature behavior of three fabricated STW delay lines on rotated Y-cut quartz. Here, the solid curves represent a spline fit to the data points shown as crosses. Our oscillator is designed for operating at approximately  $80^\circ\text{C}$  without temperature stabilization, which would raise the power consumption. The turning point temperature of the complete oscillator has been found to be shifted slightly to a lower temperature due to the temperature coefficients of the amplifiers. Thus, the  $37.5^\circ$  rotated Y-cut substrate material, which has a turnover point of about  $83^\circ\text{C}$ , has been chosen. The resulting frequency versus temperature curve of the oscillator is shown in Fig. 12.

### V. CONCLUSION

This work demonstrates the feasibility of using high-frequency STW delay lines operating at a higher harmonic as frequency controlling elements in the feedback loops of hybrid planar acoustic oscillators. These oscillators perform as well as or better than multiplied conventional bulk crystal oscillators in nearly every characteristic and offer reductions in size, weight, power, and cost. By using highly advanced analysis methods and conventional photolithographic techniques, STW filters with low insertion loss, high  $Q$ , and sufficiently small standard deviations can be

accurately designed at frequencies up to nearly 3 GHz. Direct generation of the recently standardized SONET (Synchronous Optical Network) bit frequency of 2488.32 MHz by STW oscillators seems to be possible in the near future due to the accurate filter and microwave circuit design methods. Further improvements are expected when operation at fundamental frequencies of the delay lines is feasible on a production scale. This requires mature photolithographic techniques with a line width resolution of less than 0.5  $\mu$ m. In conclusion, an experimental STW oscillator operating at 1.9805 GHz has been fabricated and analyzed. Excellent phase noise data are obtained at a high power output.

#### ACKNOWLEDGMENT

The authors would like to thank F. Lauber of Fritz Mikrowellentechnik for helpful discussions and H.-W. Wörz of Siemens Research Laboratories for his help in the noise measurements.

#### REFERENCES

- [1] T. E. Parker, "Frequency stability of surface wave controlled oscillators," in *Proc. IEEE Int. Symp. Circuits Syst.* (New York), 1978, pp. 558-562.
- [2] B. Fleischmann, W. Ruile, and G. Riha, "Rayleigh mode SAW filters on quartz for timing recovery above 1 GHz," in *IEEE Ultrasonics Symp. Proc.*, 1986, pp. 163-167.
- [3] B. Fleischmann, W. Ruile, G. Riha, and A. R. Baghai-Wadji, "Reproducible SAW-filters at 2.5 GHz," in *Proc. IERE Int. Conf. Frequency Control and Synthesis* (Guildford), 1987, pp. 29-35.
- [4] D. B. Leeson, "A simple model of feedback oscillator noise spectrum," *Proc. IEEE*, vol. 54, pp. 329-330, 1966.
- [5] T. E. Parker, "1/f phase noise in quartz delay lines and resonators," in *IEEE Ultrasonics Symp. Proc.*, 1979, pp. 878-881.
- [6] S. K. Salmon, "Practical aspects of surface-acoustic-wave oscillators," *IEEE Trans. Microwave Theory Tech.*, vol. MTT-27, pp. 1012-1018, 1979.
- [7] D. Scherer, "Design principles and test methods for low phase noise RF and microwave sources," presented at Hewlett-Packard RF and Microwave Measurement Symp., 1978.
- [8] T. E. Parker, "Current developments in SAW oscillator stability," in *Proc. 31st Annu. Frequency Control Symp.*, June 1977, pp. 359-364.
- [9] E. J. Wilkinson, "An N-way hybrid power divider," *IRE Trans. Microwave Theory Tech.*, vol. MTT-8, pp. 116-118, 1960.
- [10] RTI Ingenieurbüro für Hochfrequenztechnik, *SANA Network Analysis Program Handbook*. Munich, 1987.
- [11] K. F. Lau, K. H. Yen, A. M. Kong, and K. V. Rousseau, "SAW oscillators at 3 to 5 GHz range," in *IEEE Ultrasonics Symp. Proc.*, 1983, pp. 263-266.
- [12] M. Lewis, "Surface skimming bulk waves, SSBW," in *IEEE Ultrasonics Symp. Proc.*, 1977, pp. 744-752.
- [13] K. F. Lau, K. H. Yen, R. S. Kagiwada, and A. M. Kong, "High frequency temperature stable SBAW oscillators," in *IEEE Ultrasonics Symp. Proc.*, 1980, pp. 240-244.
- [14] A. R. Baghai-Wadji, S. Selberherr, and F. Seifert, "On the calculation of charge, electrostatic potential and capacitance in general finite SAW structures," in *IEEE Ultrasonics Symp. Proc.*, 1984, pp. 170-173.
- [15] B. Auld, *Acoustic Fields and Waves in Solids*, vol. 1. New York: Wiley, 1973, pp. 170-173.
- [16] R. L. Rosenberg, "Wave-scattering properties of interdigital SAW transducers," *IEEE Trans. Sonics Ultrason.*, vol. SU-28, pp. 26-41, Jan. 1981.
- [17] W. Ruile, F. Müller, and G. Riha, "Metal-RACs with track interference weighting," in *IEEE Ultrasonics Symp. Proc.*, 1986, pp. 147-151.
- [18] T. Nishikawa, A. Tani, C. Takeuchi, and J. Minowa, "1.6 GHz SH-type surface acoustic wave filter," *Jap. J. Appl. Phys.*, suppl. 20-4, pp. 29-32, 1981.
- [19] D. F. Thompson and B. A. Auld, "Surface transverse wave propagation under metal strip gratings," in *IEEE Ultrasonics Symp. Proc.*, 1986, pp. 261-266.
- [20] M. N. Islam, H. A. Haus, and J. Melngailis, "Bulk radiation by surface acoustic waves propagating under a grating," *IEEE Trans. Sonics Ultrason.*, pp. 123-135, Mar. 1984.
- [21] B. A. Auld and B. H. Yeh, "Theory of surface skimming SH wave guidance by a corrugated surface," in *IEEE Ultrasonics Symp. Proc.*, 1979, pp. 786-790.
- [22] A. J. De Vries, R. L. Miller, and T. J. Wojcik, "Reflection of a surface wave from three types of interdigital transducers," in *IEEE Ultrasonics Symp. Proc.*, 1972, pp. 358.
- [23] H. Engan, "Surface acoustic wave multielectrode transducers," *IEEE Trans. Sonics Ultrasonics.*, vol. SU-22, pp. 395-401, Nov. 1975.
- [24] K. F. Lau, K. H. Yen, R. S. Kagiwada, and A. M. Kong, "A temperature stable 2 GHz SBAW delay line oscillator," in *Proc. 34th Frequency Control Symp.* (Monmouth), 1980, pp. 237-242.
- [25] T. E. Parker, "Random and systematic contributions to long term frequency stability in SAW oscillators," in *IEEE Ultrasonics Symp. Proc.*, 1983, pp. 257-262.
- [26] R. L. Jungerman, R. L. Baer, and R. C. Bray, "Delay dependence of phase noise in SAW filters," in *IEEE Ultrasonics Symp. Proc.*, 1985, pp. 258-261.
- [27] R. L. Baer, D. M. Hoover, D. Molinari, and E. C. Herleikson, "Phase noise in SAW filters," in *IEEE Ultrasonics Symp. Proc.*, 1984, pp. 30-35.
- [28] S. S. Elliott and R. C. Bray, "Direct phase noise measurements of SAW resonators," in *IEEE Ultrasonics Symp. Proc.*, 1984, pp. 180-185.
- [29] E. Reese, Jr., and W. S. Ishak, "Automatic phase noise measurements using MSW-delay-line-based discriminators," in *IEEE Ultrasonics Symp. Proc.*, 1985, pp. 169-173.
- [30] P. A. Moore, S. K. Simon, "Surface acoustic wave reference oscillators for UHF and microwave generators," *Proc. Inst. Elec. Eng.*, vol. 130, pt. H, pp. 477-482, Dec. 1983.
- [31] S. J. Kerbel, "Design of harmonic surface acoustic wave (SAW) oscillators without external filtering and new data on the temperature coefficient on quartz," in *IEEE Ultrasonics Symp. Proc.*, 1974, pp. 276-281.

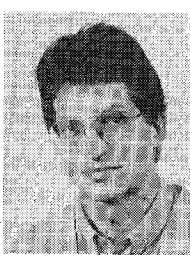
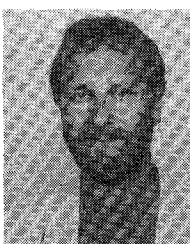
**Ludwig Eichinger** (S'88) was born in Amberg, West Germany, in 1959. He received the Dipl. Ing. degree in electrical engineering from the Technical University Munich, West Germany, in 1987.

He then joined the Work Microwave, Holzkirchen, West Germany, where he is engaged in work on microwave oscillators.



**Bernd Fleischmann** was born in Nuremberg, West Germany, in 1960. He received the Dipl. Ing. degree in electrical engineering from the Technical University Munich in 1985.

Since then, he has been with the microacoustics group of the Siemens Research Laboratories, Munich, where he is engaged in research on high-frequency surface acoustic wave filters.

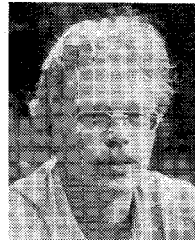




**Peter Russer** (SM'81) was born in Vienna, Austria, in 1943. He received the Dipl. Ing. degree in 1967 and the Dr. Techn. degree in 1971, both in electrical engineering and both from the Technical University Vienna, Austria.

From 1968 to 1971, he was an Assistant Professor at the Institute of Physical Electronics of the Technical University Vienna, where he carried out research work on the Josephson effect. In 1971, joined the Research Institute of AEG-Telefunken, Ulm, West Germany, where he worked on fiber-optic communication, high-speed solid-state electronic circuits, laser modulation, and fiber-optic gyroscopes. He was corecipient of the NTG-award (1979). Since January 1981, he has held the Chair of High Frequency Engineering at the Technical University Munich, West Germany. His current research interests are integrated millimeter-wave circuits, computer-aided circuit design, microwave oscillators, and optical communications.

Dr. Russer is a member of the Austrian Physical Society (ÖPG), the German Physical Society (DPG), and the Nachrichtentechnische Gesellschaft (NTG), Germany.



**Robert Weigel** (S'88) was born in Ebermannstadt, West Germany, in 1956. He received the Dipl. Ing. degree in electrical engineering from the Technical University Munich, West Germany, in 1982. Since then, he has been working as a Research Assistant at the Technical University Munich, where he is studying towards the Dr. Ing. degree in electrical engineering. His research deals with integrated optics and surface acoustic waves.